Available online at www.eccomasproceedia.org
Eccomas Proceedia COMPDYN (2023) 2238-2248

ECCOMAS
Proceedia

COMPDYN 2023
9th ECCOMAS Thematic Conference on
Computational Methods in Structural Dynamics and Earthquake Engineering
M. Papadrakakis, M. Fragiadakis (eds.)
Athens, Greece, 12-14 June 2023

DISPLACEMENT-BASED DESIGN OF HYSTERETIC DAMPERS FOR SEISMIC RETROFIT OF FRAMES

Eleonora Bruschi[1], Virginio Quaglini[1], and Luca Zoccolini[1]

[1] Politecnico di Milano
Piazza Leonardo da Vinci 32, 20133, Milano
{eleonora. bruschi, virginio.quaglini, luca.zoccolini}@polimi.it

Abstract

A simple and affordable displacement-based design procedure for the seismic rehabilitation of frame structures equipped with hysteretic dampers has been recently proposed in the literature. The method is based on the Capacity Spectrum Method and is developed in the acceleration-displacement response spectrum (ADRS) space. The procedure calculates the properties of the dampers required to achieve the desired structural performance in compliance with the assumed limit states. The required performance is expressed in terms of a target displacement demand, and the structural response is achieved by reducing the demand response spectrum as a function of the additional damping introduced by the supplementary energy dissipation. Iterations are required since the addition of hysteretic dampers increases the stiffness of the system; however, convergence is reached in very few steps.

The present work aims at assessing the use of the procedure for the seismic retrofit of two existing structures taken as case-studies. One building is a 4-story residential RC structure designed according to outdated codes that ignored seismic actions, while the second building is a 4-story steel-framed structure designed according to old-code MRFs considering gravity loads and low earthquake-induced loads. The upgrade of both structures is performed in order to achieve an assigned ductility factor for the main frame μ_F in the range 1 - 1.5. Attention is also paid to limit the increase in axial force induced in the columns by the dampers in order to avoid buckling issues.

To check the accuracy of the design procedure, non-linear static analyses are performed, showing a satisfactory agreement between the global performance and the design target. Non-linear dynamic analyses are eventually carried out considering a suite of bidirectional artificial ground motions in accordance with the provisions of the Italian and European building codes.

Keywords: Hysteretic damper, Energy dissipation, Reinforced concrete, Steel frame, Seismic Upgrade, Non-linear analyses, OpenSees.

ISSN:2623-3347
Peer-review under responsibility of the organizing committee of COMPDYN 2023.
doi: 10.7712/120123.10556.20310

1 INTRODUCTION

The preservation of the building heritage from natural disasters, such as earthquakes, is an open discussed issue in Europe. In particular, Italy is a country prone to seismic activity, and recently many strong earthquakes occurred in the territory (e.g., Abruzzo 2009, Emilia Romagna 2012, Centre of Italy 2016). These natural disasters caused many losses in terms of human lives but also significant damage to buildings.

In the last decades many techniques for retrofitting existing structure have been proposed, which are able to reduce the probability of failure and prevent structural damage. Among them, the supplementary energy dissipation is an appealing one. This technique can be applied to both existing and new structures and it is realized through dampers, able to dissipate the seismic energy, that are inserted within steel braces installed between consecutive floors. The presence of the damped braces allows to increase the structural stiffness, with a consequent reduction of displacements, and dissipate the seismic energy.

Even if the use of energy dissipation devices has been proved to be effective in reducing the seismic effects on both reinforced concrete (RC) [1–8] and steel structure [8–10], the implementation of these systems for ordinary buildings is not widely used. The practitioners still have little confidence in using energy dissipation strategies and one the reasons is the lack of an easy adoptable design procedure. [9]

Some Authors of this work have recently proposed a displacement-based design procedure, which allows to easily compute the characteristics of the dissipative devices to reach a desired performance level during a seismic event [11–13]. The dissipative brace system, represented by a simple Single Degree of Freedom system (SDOF), is dimensioned by means of an iterative procedure based on the Capacity Spectrum Method [14,15]. Even if there are other similar methods able to compute the properties of those devices [16–20] the peculiarity of this method is its simplicity. At the first iteration of the procedure, a single non-linear static analysis is performed to evaluate the capacity curve of the bare structure, while in the subsequent iterations, the pushover curve of the upgraded frame is computed by means of simple analytical equations accounting for the stiffness and the strength of the damped bracing system. The iterative procedure can be graphically represented in the Acceleration-Displacement Response Spectra (ADRS) plane giving the opportunity to visualize for each iteration the demand and the upgraded capacity. At the end, analytical equations are used to determine the strength and stiffness of the dampers at each floor of the structure. These properties are computed such that the displacement profile of the upgraded structure matches the one of the first mode of the original structure [17].

The procedure can be implemented in a spreadsheet, and usually ends in few steps. In addition to that, it must be mentioned that this method has been developed with explicit consideration of the Italian Building Code (NTC2018) [21,22] and the Eurocode [23].

The present study aims at showing the ease and effectiveness of the procedure presented by Bruschi et al. [11]; in particular, it has been applied to two mid-rise buildings designed according to old regulations. The first one is a 4-story RC residential building [18] and the other one is a 4-story steel moment-resisting frame (MRF) [9,10]. The properties of the damped bracing system are computed to satisfy the ultimate limit state according to the provisions provided by the NTC2018 [21], and non-linear analyses have been computed to validate the behavior of the upgraded structures.

2 DESCRIPTION OF THE CASE-STUDIES

The first case-study structure is a 4-story RC building located in Potenza (Italy), which is defined as medium/high seismicity area according to NTC2018 [21], and it is characterized by a peak ground acceleration (PGA) of 2.45 m/s^2. The structure is assumed to be funded on soil type B with a topographic factor T_1 [18]. The dimensions of the structure are shown in Figure 1; information on materials, reinforcement, and loads are reported in reference [11,18]. The structural members were designed considering vertical loads only, therefore, they are not dimensioned for the effect of the earthquakes.

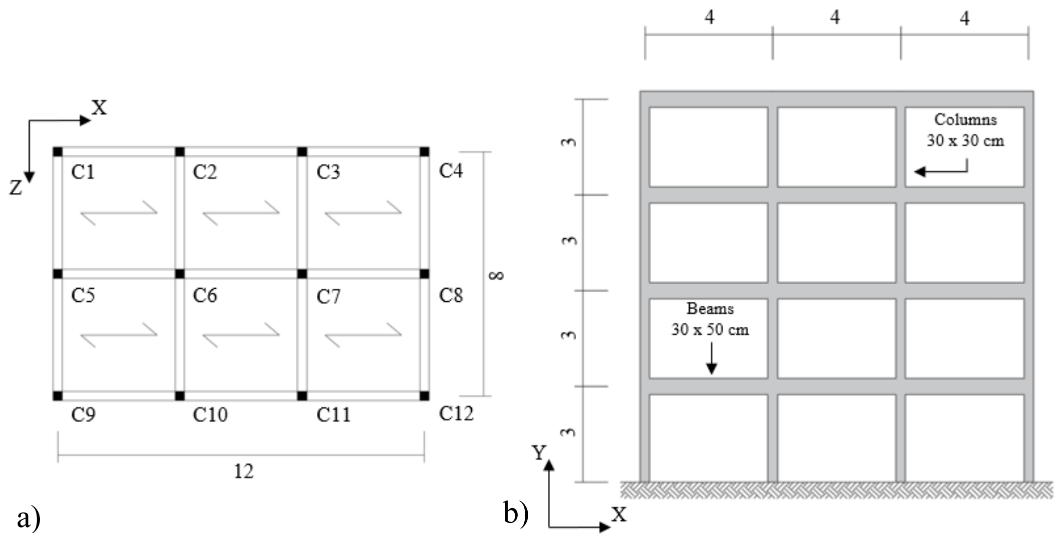

Figure 1: Existing RC building in Potenza: (a) plan view and (b) elevation view [11]

The second analyzed structure is a 4-story steel MRF [9,10], which is shown in Figure 2. The building was designed without considering the requirement of similar resistance and stiffness in both main directions introduced in current regulations [20-22], indeed it is characterized by the same orientation of the columns, which results in higher stiffness and strength in the Z-direction. Moreover, both gravity and low earthquake-induced loads corresponding to a spectrum for soil A and PGA equal to 1.96 m/s^2 were considered in the design. Detailed information on the masses and gravity loads are reported in reference [10].

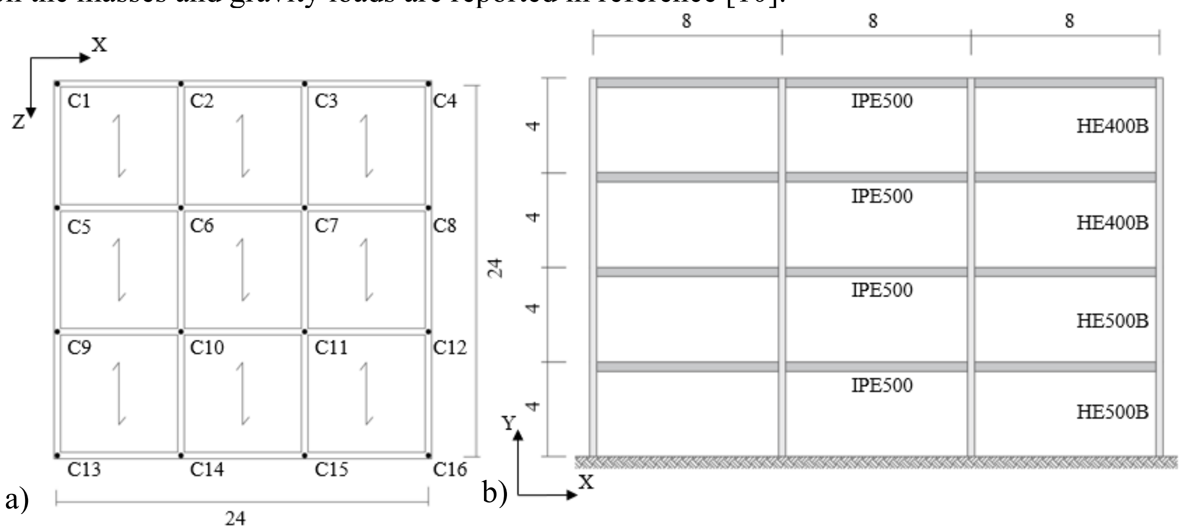

Figure 2: Existing steel MRF building: (a) plan view and (b) elevation view [8]

3 NUMERICAL MODEL IN OPENSEES

A 3D finite element model of both case-studies was developed in the OpenSees framework [24,25]. The columns of the two structures were modeled with fixed supports at the ground level, simulating rigid foundations. The floor slabs were modeled as rigid diaphragms, therefore, the nodes belonging to the same floor have the same displacement of the center of mass, where the mass of the floor, computed according to the NTC2018 [21], was concentrated. Dead and live loads were defined according to the tributary area concept and were uniformly applied on the beams following the direction of the floor slabs shown in Figure 1 and Figure 2.

The *forceBeamColumn* element object [24] was implemented for both columns and beams. This type of element is divided into three distinct sub-elements: two-external parts of length L_{pl}, defined as plastic hinges, in which the non-linear behavior is modeled through a fiber section model, and a central linear elastic part. The length of the non-linear external sub-elements assumes different values for the RC (Eq. 1) and steel MRF (Eq. 2).

$$L_{pl} = \frac{z}{30} + 0.2h + 0.11\left(\frac{d_b f_y}{\sqrt{f_c}}\right) \tag{1}$$

Eq. (1) is the expression reported in the Eurocode 8 [23], where z is the shear span of the structural element, h is the depth of the section, d_b is the diameter of the longitudinal reinforcement, f_y is the yield strength of steel and f_d is the compressive strength of concrete. Eq. (1) can be used only if a well-detailed confinement model of concrete is assumed. The concrete was modeled with the library uniaxial material *Concrete04* [24] and each reinforcement bar, represented by a single fiber, was defined through the material model with isotropic strain hardening *Steel02* [24]. A detailed description of the adopted model is reported in [26,27].

Eq. (2) was used to define the length of the plastic regions for the steel MRF [28], where L_v is the shear length of the steel element.

$$L_{pl} = 0.22 \cdot L_v \tag{2}$$

Even for the steel MRF the *Steel02* material model with isotropic strain hardening [24] was implemented, and detailed information is reported in reference [9].

P-Delta effects were considered in the analyses. The structural damping of the frames was modeled as a function of the tangent stiffness matrix only: for the RC frame an equivalent damping ratio of 5% was used [2,11,12] while for the steel MRF, 3% was the selected value [9,29,30]. Infill panels were not modeled and since their contribution was already accounted in the equivalent damping.

In the RC frame model, an “axial buffer”, defined by a *zeroLength* element object [24], was placed between one end of each beam and the adjacent node, in order to eliminate the fictitious axial force that is generated by the interaction between the fiber section of the beam element and the rigid diaphragm [31].

4 DESIGN OF THE SEISMIC REHABILITATION

The applied displacement-based design procedure aims at proportioning the damped bracing system to achieve a target structural performance. A detailed explanation of the procedure is reported in the work of Bruschi et al. [11]. The method is developed in the ADRS space and the damped brace (DB) capacity curve is obtained as the difference between the capacity curve of the Frame + Damped Brace (F+DB) system achieving the target displacement d_p, and the capacity curve of the bare frame (F). Then, the mechanical properties of the identified equivalent SDOF damped brace are distributed at each story according to a proportionality criterion with respect to the first mode properties of the unbraced frame. It is necessary to recall that a pre-requisite for the application of the procedure is that the behavior of the frame building is governed by the first mode, which legitimates the condensation of the Multi Degree of Freedom (MDOF) structure to the equivalent SDOF system.

The two structures were retrofitted to satisfy the life-safety limit state (SLV) provided by the NTC2018 [21]. As previously reported, the RC structure was upgraded according to the seismic hazard associated with the municipality of Potenza, considering a functional class c_u = II and nominal life V_n = 50 years. The properties of the dissipating devices of the steel MRF were computed to upgrade the seismic performance of the building to comply with larger seismic demand; therefore, the considered seismic hazard corresponds to the municipality of Lamezia Terme (Italy), PGA =4.47 m/s^2, soil type C, topographic factor T_1, functional class c_u = II and nominal life V_n = 100 years.

In the RC concrete structure, the procedure was separately applied to both X- and Z- directions, while it was applied only to the X-direction in the steel MRF, due to the preferred orientation of the column sections with their strong axis aligned in the Z-direction. The bilinear curves of the equivalent SDOF systems of the two as-built structures were determined from the modal capacity curves. The target displacement d_p for the RC structure was defined as the ending point of the elastic branch on the pushover curve, in this way the immediate occupancy structural performance level was guaranteed [32]. On the contrary, the performance point for the steel MRF was defined as the elastic limit of the pushover curve (d_y) multiplied by the ductility factor μ_F = 1.5 in agreement with the reference [10]. Table 1 and Table 2 show the parameters of the equivalent bilinear capacity curve of the two structures.

Table 1: Properties of the equivalent SDOF system and bilinear capacity curves of RC structure

Direction	$\Gamma\,[-]$	$m^*[ton]$	$d_y^*\,[m]$	$V_y^{*F}\,[kN]$	$d_p^*\,[m]$	$V_p^{*F}\,[kN]$	ξ_F [%]
X	1.27	340	0.012	182	0.036	388	5.7
Z	1.27	339	0.012	186	0.036	385	6.4

Table 2: Properties of the equivalent SDOF system and bilinear capacity curves of steel MRF

Direction	$\Gamma\,[-]$	$m^*[ton]$	$d_y^*\,[m]$	$V_y^{*F}\,[kN]$	$d_p^*\,[m]$	$V_p^{*F}\,[kN]$	ξ_F [%]
X	1.27	1020	0.120	1381	0.183	1825	6.4
Z	1.31	994	0.134	3307	0.203	3967	10.9

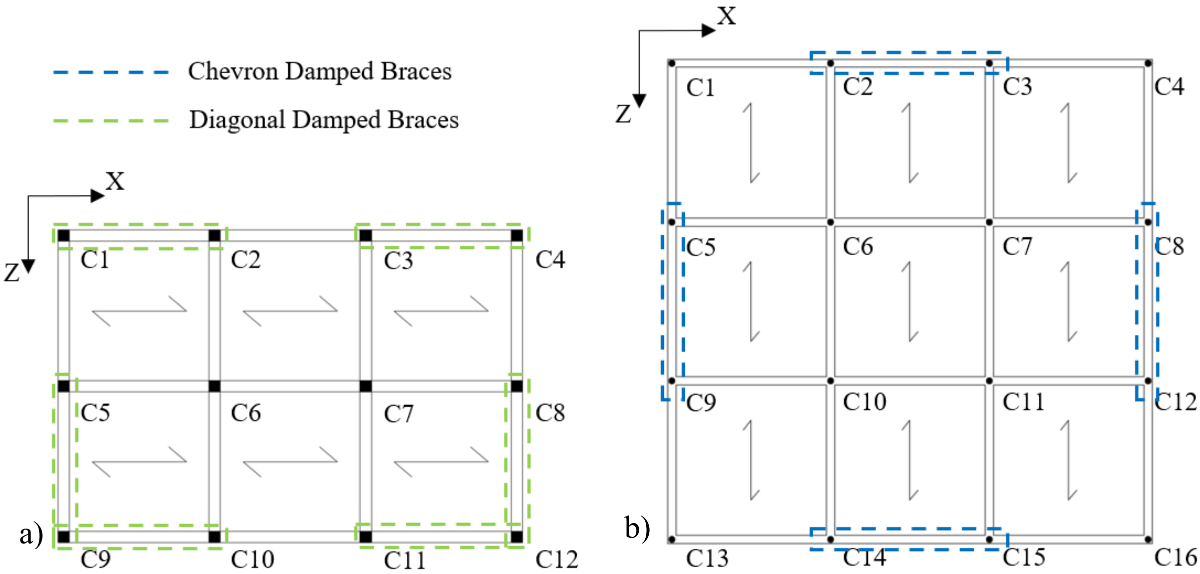

Figure 3: Plan layout of damped braces: (a) RC structure; (b) steel MRF.

The retrofit of the two structures was performed by using steel braces, equipped with hysteretic devices with ductility level μ_{DB} = 10 and κ_{DB} = 1.0, which corresponds to an equivalent viscous damping ratio of ξ_{DB} = 57.3%. The braces were inserted in the facades of the RC frame with a diagonal configuration, while a chevron configuration was adopted for the case of the steel MRF. Figure 3 shows the plan layout of the damped braces in the two structures. The properties of the dampers at each floor of the RC and steel structures are listed in Table 3 and Table 4 respectively.

Table 3: Properties of the damped brace of the RC structure

Story	X-Direction		Z-Direction	
	K_i^{DB} $[kN/mm]$	N_{yi}^{DB} $[kN]$	K_i^{DB} $[kN/mm]$	N_{yi}^{DB} $[kN]$
1^{st}	67.4	77.0	62.6	73.0
2^{nd}	56.1	68.0	51.5	64.1
3^{rd}	55.5	48.6	51.0	46.0
4^{th}	53.3	22.3	47.6	21.1

Table 4: Properties of the damped brace of the steel MRF

Story	X-Direction	
	K_i^{DB} $[kN/mm]$	N_{yi}^{DB} $[kN]$
1^{st}	187.9	516.8
2^{nd}	130.6	466.6
3^{rd}	118.0	351.4
4^{th}	111.9	182.5

5 NUMERICAL INVESTIGATION

The effectiveness of the design was validated by performing both non-linear static analyses (NLSAs) and non-linear dynamic analyses (NLDAs). Figure 4 shows the capacity curves along the X-direction of the as-built and upgraded structures plotted in the ADRS plane and compared with the response demand curve for the relevant damping. It can be seen how the capacity curves of both case-study structures meet the demand curves at the target displacement. The equivalent SDOF system equipped with the damped brace satisfies the required performance level. For the sake of conciseness, the results in Z-direction are not reported.

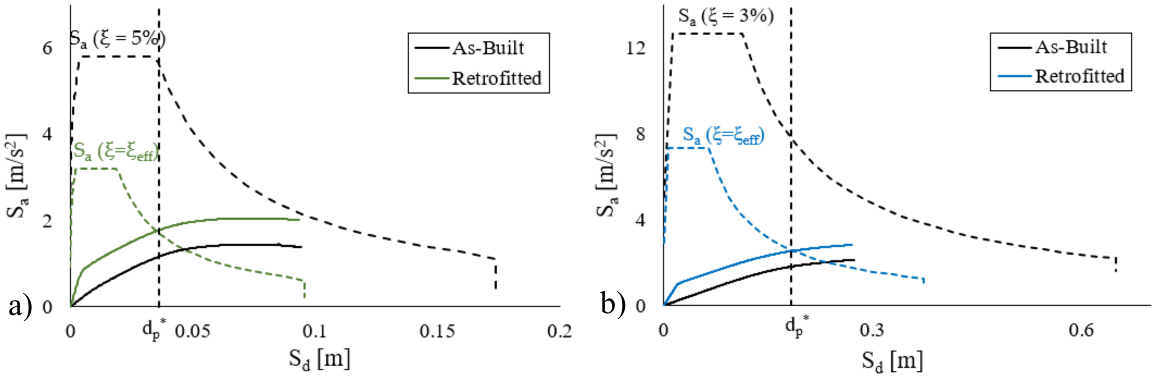

Figure 4: Results of NLSAs in X-direction: (a) RC structure; (b) steel MRF

NLDAs were performed in conformity with the NTC2018 [21], considering two sets of seven artificial ground motions, compatible with the response spectrum, defined by NTC2018 [21] of the two sites where the buildings are placed. The ground motions were generated by the software SIMQKE [33]. Figure 5 compares the capacity curves of the as-built and the upgraded structures with average maximum top displacement and base shear force (AVG TH) obtained from the NLDAs. The results of the NLDAs are in excellent agreement with the ones from the NLSAs, since the average values (labelled as “AVG”) practically lay on the capacity curves. Indeed, for a same displacement, base shear values obtained by the NLDAs are similar to the base shear of the capacity curve.

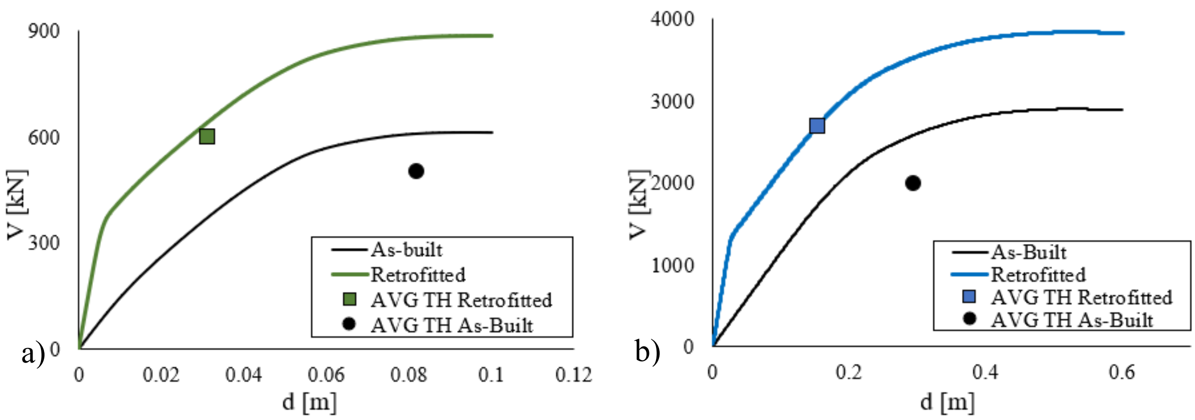

Figure 5: Comparison between NLSAs and NLDAs: (a) RC structure; (b) steel MRF

Usually, the introduction of hysteretic devices inside a structure reduces the lateral deformation but increases the shear force at the floors with respect to the original structure. Figure 6 shows the increment of the shear force at each floor of the RC structure. The forces of the upgraded structure are slightly higher than that the bare structure, with a difference lower than 10% at each floor.

Similar results were obtained also for the steel MRF. It is worth mentioning that an important issue for steel structures concerns the buckling of the columns that are subjected to higher axial forces transferred by the braces. Therefore, the compressive axial force in the columns adjacent to the Chevron braces was computed at each floor and divided by its buckling load ($N_{buckling}$), evaluated according to the NTC2018 [21]. Figure 7 shows the check performed on the most stressed column of the steel case-study, which is the column C2 according to Figure 3. The value of the normalized axial force ($N/N_{buckling}$) is less than unity at each floor, therefore the buckling limitation requirement is satisfied.

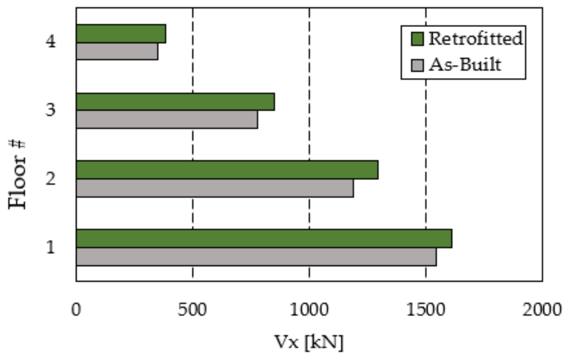

Figure 6: Comparison of maximum shear force at each floor obtained by bidirectional NLDAs with and w/o damped braces

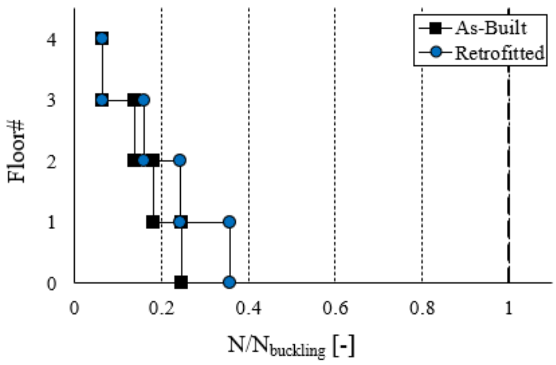

Figure 7: Buckling checks in the most stressed columns in the steel MRF (column C2)

6 CONCLUSIONS

The present work focuses on the evaluation of a handy-to-use design procedure for the seismic rehabilitation of frame structures equipped with hysteretic dampers. The procedure is suitable for professional applications thanks to its simplicity. Indeed, it requires performing a single NLSA on the bare frame at the beginning of the process, to determine the capacity curve of the structure, which is then identified through simple analytical equations. In this way, the procedure can be implemented in a spreadsheet, and it converges in very few steps. The proposed design method is applicable to low- and mid-rise structures with regular distribution of masses and stiffnesses in plan and in elevation.

To demonstrate the effectiveness of this method, two case studies, a 4-story RC structure and a 4-story steel MRF, were investigated. In case of RC case-study structure, the purpose of the retrofit design was to keep the building in the elastic regime, while the damped brace system of the steel MRF was designed to allow a controlled inelastic deformation of the structure. The effectiveness and reliability of the proposed procedure was assessed by evaluating the seismic performance of the upgraded buildings in static and dynamic non-linear analyses. The retrofitted structures met the target performance, showing a consistent reduction of lateral deformation with respect to the bare configuration, without an excessive increase in terms of internal forces.

It is worth mentioning that there are still some limitations in this study and further investigations are required in order to make the procedure more general. In particular, in the current form, the procedure considers only structures that are regular in plan and in elevation. In future studies, the method will be extended also to in-elevation irregular buildings and unsymmetric-plan arrangements.

REFERENCES

[1] V. Quaglini, C. Pettorruso, E. Bruschi, Design and Experimental Assessment of a Prestressed Lead Damper with Straight Shaft for Seismic Protection of Structures, *Geosciences* (Switzerland), **12**, 2022. https://doi.org/10.3390/geosciences12050182.

[2] E. Bruschi, V. Quaglini, Assessment of a novel hysteretic friction damper for the seismic retrofit of reinforced concrete frame structures, *Structures*, **46**, 793–811, 2022. https://doi.org/10.1016/j.istruc.2022.10.113.

[3] C. Pettorruso, E. Bruschi, V. Quaglini, Supplemental energy dissipation with prestressed Lead Extrusion Dampers (P-LED): Experiments and modeling, *8th ECCOMAS Thematic Conference on Computational Methods in Structural Dynamics and Earthquake Engineering,* Athens, Greece, 28-30 June, 2021.

[4] V. Quaglini, E. Bruschi, Controllo passivo mediante controventi dissipativi. Principi generali, requisiti normativi ed evoluzione dei principali dispositivi a comportamento dipendente dallo spostamento, *Structural*, **240**, 09, 2022. https://doi.org/10.12917/STRU240.09.

[5] V. Quaglini, E. Bruschi, C. Pettorruso, M. Sartori, Design and experimental assessment of a novel damper with high endurance to seismic loads, *Procedia Structural Integrity*, **44** (2023) 1451–1457. https://doi.org/10.1016/j.prostr.2023.01.186.

[6] E. Bruschi, V. Quaglini, Numerical investigation on the seismic performance of a RC framed building equipped with a novel Prestressed LEad Damper with Straight Shaft, *Procedia Structural Integrity,* **44**, 1443–1450, 2023. https://doi.org/10.1016/j.prostr.2023.01.185.

[7] V. Quaglini, C. Pettorruso, E. Bruschi, Experimental and numerical assessment of prestressed lead extrusion dampers, *International Journal of Earthquake Engineering*, **XXXVIII**, 46–69, 2021.

[8] E. Bruschi, L. Zoccolini, S. Cattaneo, V. Quaglini, Experimental Characterization, Modeling, and Numerical Evaluation of a Novel Friction Damper for the Seismic Upgrade of Existing Buildings, *Materials*, **16**, 1933, 2023. https://doi.org/10.3390/ma16051933.

[9] E. Bruschi, V. Quaglini, L. Zoccolini, Seismic Upgrade of Steel Frame Buildings by Using Damped Braces, *Applied Sciences*, **13**, 2063, 2023. https://doi.org/10.3390/app13042063.

[10] E. Gandelli, D. de Domenico, V. Quaglini, Cyclic engagement of hysteretic steel dampers in braced buildings: a parametric investigation, *Bulletin of Earthquake Engineering*. **19**, 5219–5251, 2021. https://doi.org/10.1007/s10518-021-01156-3.

[11] E. Bruschi, V. Quaglini, P.M. Calvi, A simplified design procedure for seismic upgrade of frame structures equipped with hysteretic dampers, *Engineering Structures,* **251**, e113504, 2021. https://doi.org/10.1016/j.engstruct.2021.113504.

[12] E. Bruschi, V. Quaglini, P.M. Calvi, A simplified design procedure to improve the seismic performance of RC framed buildings with hysteretic damped braces, *New Metropolitan Perspectives 2022 - 5th International Symposium "Post COVID Dynamics: Green and Digital Transition, between Metropolitan and Return to Villages' Perspectives"*, Reggio Calabria, Italy, 25-27 May 2022, Volume 482 LNNS, pp. 2173 – 2182, ISBN: 978-3-031-06825-6.

[13] V. Quaglini, C. Pettorruso, E. Bruschi, Dimensionamento di dispositivi dissipativi per la riabilitazione sismica di strutture intelaiate, *Structures*, **e237**, 2021. https://doi.org/10.12917/STRU237.25.

[14] P. Fajfar, Capacity spectrum method based on inelastic demand spectra, *Earthquake Engineering and Structural Dynamics,* **28**,979–993, 1999 . https://doi.org/10.1002/(SICI)1096-9845(199909)28:9<979::AID-EQE850>3.0.CO;2-1.

[15] R.W. Niewiarowski, C. Rojahn, Seismic Evaluation and Retrofit of Concrete Buildings, Redwood City, CA, USA, 1996.

[16] I. Nuzzo, D. Losanno, N. Caterino, Seismic design and retrofit of frame structures with hysteretic dampers: a simplified displacement-based procedure, *Bulletin of Earthquake Engineering*, **17**, 2787–2819, 2019. https://doi.org/10.1007/s10518-019-00558-8.

[17] F. Mazza, A. Vulcano, Displacement-based design procedure of damped braces for the seismic retrofitting of r.c. framed buildings, *Bulletin of Earthquake Engineering*, **13**, 2121–2143, 2015. https://doi.org/10.1007/s10518-014-9709-7.

[18] A. di Cesare, F.C. Ponzo, Seismic Retrofit of Reinforced Concrete Frame Buildings with Hysteretic Bracing Systems: Design Procedure and Behaviour Factor, *Shock and Vibration*, **2017**, 2017. https://doi.org/10.1155/2017/2639361.

[19] F. Mazza, M. Mazza, A. Vulcano, Displacement-based seismic design of hysteretic damped braces for retrofitting in-elevation irregular RC framed structures, *Soil Dynamics and Earthquake Engineering*, **69**, 115–124, 2015. https://doi.org/10.1016/j.soildyn.2014.10.029.

[20] A. v. Bergami, C. Nuti, A design procedure of dissipative braces for seismic upgrading structures, *Earthquake and Structures*, **4**, 85–108, 2013. https://doi.org/10.12989/eas.2013.4.1.085.

[21] Italian Council of Public Works, *Technical Standards on Constructions*, Rome, Italy, 2018.

[22] Italian Council of Public Works, *Commentary on the Technical Standards on Constructions*, Rome, Italy, 2019.

[23] EN 1998–3, *Design of Structures for Earthquake Resistance - Part 3: Assessment and Retrofitting of Buildings*, British Standards Institution, Brussels, Belgium, 2005.

[24] F. McKenna, G.I. Fenves, M.H. Scott, Open System for Earthquake Enguneering Simulation, (2000).

[25] OpenSeesWiki online manual, Available online: https://opensees.berkeley.edu/wiki/index.php/Main_Page, (n.d.).

[26] E. Bruschi, P.M. Calvi, V. Quaglini, Concentrated plasticity modelling of RC frames in time-history analyses, *Engineering Structures*, **243**, 112716, 2021. https://doi.org/10.1016/j.engstruct.2021.112716.

[27] E. Bruschi, V. Quaglini, P.M. Calvi, Numerical assessment of concentrated plasticity models of ductile RC frames in non-linear dynamic analyses, *2nd Fib Italy YMG Symposium on Concrete and Concrete Structures*, Rome, Italy, November 18-19, 2021.

[28] M. Bosco, L. Tirca, Numerical simulation of steel I-shaped beams using a fiber-based damage accumulation model, *Journal of Constructional Steel Research*, **133**, 241–255, 2017. https://doi.org/10.1016/j.jcsr.2017.02.020.

[29] T. Sullivan, T. Maley, G.M. Calvi, Seismic response of steel moment resisting frames designed using a Direct DBD procedure, *EURODYN 2011 (Ed.), Proceedings of the 8th International Conference on Structural Dynamics*, Leuven, Blegium, July 4-6, 2011.

[30] M.J.N. Priestley, G.M. Calvi, M. Kowalsky, *Displacement-based seismic design of structures*, Pavia, 2007.

[31] F. Barbagallo, M. Bosco, E.M. Marino, P.P. Rossi, On the fibre modelling of beams in RC framed buildings with rigid diaphragm, *Bulletin of Earthquake Engineering*, **18**, 189–210, 2020. https://doi.org/10.1007/s10518-019-00723-z.

[32] F.C. Ponzo, A. di Cesare, A. Telesca, A. Pavese, M. Furinghetti, Advanced modelling and risk analysis of rc buildings with sliding isolation systems designed by the italian seismic code, *Applied Sciences (Switzerland),* **11,** 1–16, 2021. https://doi.org/10.3390/app11041938.

[33] SIMQKE (SIMulation of earthQuaKE ground motions), Available online: https://gelfi.unibs.it/software/simqke/simqke_gr.htm , (n.d.).